Hindawi
Science and Technology of Nuclear Installations
Volume 2023, Article ID 8322393, 9 pages
https://doi.org/10.1155/2023/8322393

Research Article

Simulations of Core Damage Progression for TMI-2 Severe Accident Using CINEMA Computer Code

Rae-Joon Park,[1] **Donggun Son,**[1] **Jun Ho Bae,**[1] **Sung Won Bae,**[1] **Bub-Dong Chung,**[2] **and Kwang Soon Ha**[1]

[1]*Korea Atomic Energy Research Institute, 1045 Daedeok-daero, Yuseong-Gu, Daejeon 34039, Republic of Korea*
[2]*FNC Technology, 593 Daedeok-daero, Yuseong-Gu, Daejeon 34112, Republic of Korea*

Correspondence should be addressed to Rae-Joon Park; rjpark@kaeri.re.kr

Received 28 October 2022; Revised 25 January 2023; Accepted 7 February 2023; Published 27 February 2023

Academic Editor: Han Zhang

As an integrated computer code development for severe accident sequence analysis in Korea, CINEMA has been developing from an initiation event to a containment failure. The CINEMA computer code is composed of CSPACE, SACAP, and SIRIUS, which are capable of simulating core melt progression with thermal hydraulic analysis of the RCS (reactor coolant system), severe accident analysis of the containment, and fission product analysis in the vessel and the containment, respectively. The severe accident progression in TMI unit 2 has been analyzed as a part of a validation of the CINEMA computer code. This analysis has been performed to validate CINEMA models on the core melt progression, in particular, RCS thermal hydraulic behavior during core melt progression, fuel cladding oxidation with hydrogen generation, and fuel melting with relocation to the lower part of the core. The CINEMA results on main parameters, such as RCS pressure and an integrated hydrogen generation mass are compared with the TMI-2 data. The CINEMA results have shown that the RCS pressure is very similar to the TMI-2 data. The CINEMA results and measured total hydrogen production are very similar, which were approximately 465 kg and 460 kg, respectively.

1. Introduction

As an integrated severe accident computer code development in Korea, CINEMA (Code for INtegrated severe accidEnt Management Analysis) has been developing for a severe accident sequence analysis from an initiation event to a containment failure [1]. The objective of this code development is to have a Korean severe accident sequence analysis code by using the existing domestic DBA (design basis analysis) code system for the severe accident sequence analysis. Figure 1 shows the code structure of the CINEMA. The CINEMA computer code is composed of CSPACE [2], SACAP (Severe Accident Containment Analysis Package) [3], and SIRIUS (SImulation of Radioactive nuclide Interaction Under Severe accident) [4], which are capable of simulating core melt progression with thermal hydraulic analysis of the RCS (reactor coolant system), severe accident analysis of the containment, and fission product analysis, respectively. The CSPACE is divided into the SPACE (Safety and Performance Analysis CodE for nuclear power plants) and the COMPASS (COre Meltdown Progression Accident Simulation Software) models, which is to calculate an overall RCS thermal hydraulic response during core melt progression in SPACE computer code [5–7] and an in-vessel melt progression to reactor vessel failure in COMPASS computer code [8, 9].

Many computer codes have been developed for the safety analysis including the severe accident, such as MELCOR [10, 11], MAAP5 [12] in USA, and ASTEC [13] in France for a severe accident sequence analysis. Many accident analysis have been performed to analyze accident progression and general reactor safety problems [14–18] and to solve the specific thermal hydraulic issues on the safety analysis including the severe accident, such as natural circulation, external reactor vessel cooling, reactor vessel cooling, and so on [19–22]. These results may be used to solve the nuclear license issues for a large power reactor and small reactors.

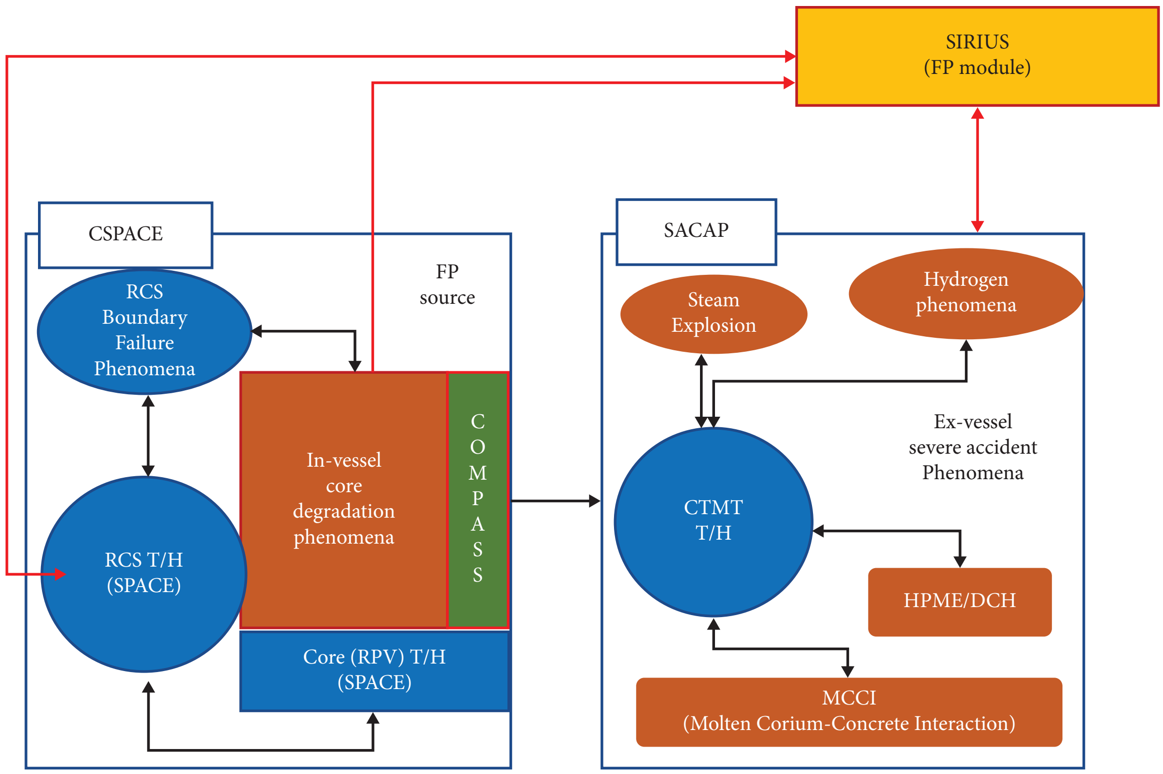

Figure 1: Structure of CINEMA computer code.

As a part of a validation of the CINEMA computer code, the TMI-2 (Three Mile Island unit 2) core melt progression has been analyzed. At first, the steady state simulation was performed to validate the CINEMA input model for TMI-2 by a comparison of the CINEMA results with a TMI-2 operating condition. After this, the transient of the TMI-2 severe accident has been analyzed to validate CSPACE modes of the CINEMA computer code on the core melt progression in-vessel, in particular, RCS thermal hydraulic behavior during core melt progression, fuel cladding oxidation with hydrogen generation, and fuel melting with relocation to the lower part of the core. The CINEMA results on main parameters, such as a pressurizer pressure and an integrated hydrogen generation mass have been compared with the TMI-2 severe accident data. In addition, the mass flow rate through the pressurizer PORV (Pilot Operated Relief Valve), which is an RCS coolant loss location, collapsed water levels in the pressurizer and the core, and the fuel rod temperature and mass in the TMI-2 severe accident have been analyzed using the CINEMA computer code.

2. Detailed Description of TMI-2 Severe Accident

A severe accident including in-vessel melt progression with corium relocation to the lower plenum of the reactor vessel occurred in the TMI-2 PWR (pressurized water reactor) on March 28, 1979 [23, 24]. Many analyses on the TMI-2 severe accident were performed using many computer codes, such as MELCOR and SCDAP/RELAP5 [25, 26]. The initiating event for TMI-2 severe accident was a TLOFW (total loss of feed water) with a SBLOCA (small break loss of coolant accident) that resulted in a significant cladding oxidation, a partial melting of the core material, a significant release of fission products from the fuel, and melted core material relocation to the lower plenum. The TMI-2 severe accident was terminated by a coolant injection into the in-vessel using the HPI (high pressure injection) water of the ECCS (emergency core cooling system). The following four main phases occurred during the TMI-2 severe accident.

(i) *Phase 1*. The initiating event of the total loss of feed water with the SBLOCA through the pressurizer PORV from 0 s to 4,440 s. This phase includes an operation and stop of the HPI, an operation of the makeup pump, and shutdown of the RCP. In this phase, boiling and two phase flow occurred in the core region.

(ii) *Phase 2*. Heat up and melting of the fuel rod by core uncover 4,440 s to 10,440 s. All RCP shutdown and core uncover occurred, which resulted in the fuel cladding oxidation and fuel melting, and relocation of the melted core material to the lower part of the core.

(iii) *Phase 3*. Core reflood by an operation of the RCP and HPI from 10,440 s to 13,440 s. This phase includes the initial core quenching by a restart of the RCP from 10,440 s to 11,580 s. The melted core material was quenched by the HPI water on the operation of feed and bleed for the RCS. In spite of this, the melted core material was relocated to the lower head in the reactor vessel.

(iv) *Phase 4*. Core relocation to the lower plenum of the reactor vessel and cooling in-vessel from 13,440 s to 18,000 s. This phase represents that the central region of the partially melted fuel was not coolable by HPI water because the corium pool with crust formation was generated in the middle of the core region. Between 13,440 s and 13,560 s, the crust in the corium pool was failed, which resulted in corium relocation to the lower plenum of the reactor vessel. However, the relocated molten material was quenched by coolant in the reactor vessel at this phase.

Table 1 shows detailed main events in the TMI-2 severe accident. This accident was initiated by the TLOFW which led to a pressure increase in the secondary and primary systems followed by turbine and main feedwater pump trip at 0 s (second). Pressure increase in the primary system caused the opening of the pressurizer PORV by a high pressure opening set point of 15.5 MPa. The reactor was tripped by a high pressurizer pressure signal. The pressurizer PORV was not closed when the pressurizer pressure was reached 15.2 MPa, which was the closed set point. Unknown to the operators, the pressurizer PORV failed to close and started the SBLOCA. The break location was the top of the pressurizer. The 1 (of 3) makeup pump 1B was operated at 41 s. The HPI (high pressure injection) was operated by high pressurizer pressure signal at 122 s. However, this pump was stopped by the operator because of a misreading of the high level of the pressurizer at 278 s. The auxiliary feedwater was startup at 480 s. Boiling occurred in the core at 552 s. The B-loop and A-loop RCP (reactor coolant pump) *s* were stopped at 4,440 s and 6,000 s, respectively. The core was uncovered at 6,184 s, which resulted in an increase of the fuel cladding temperature. The fuel cladding oxidation begun at 7,442 s. The fuel cladding was failed by overstrain at 7,719 s. The operator closed the block valve in PORV pipe line at 8,340 s, which meant the end of the SBLOCA. However, the fuel was melted at 9,014 s. One B-loop RCP was operated to supply the coolant into the core at 10,440 s. This pump was stopped at 11,580 s. The feed and bleed operation of the primary system was started to cooldown the core at 12,000 s. However, the melted core material relocated to the lower head at 13,440 s because of the molten pool formation with crust formation in the core. The general emergency declared at 18,000 s.

Figure 2 shows the end state of TMI-2 severe accident [26]. Approximately, 62 tons of the all core material was melted in the core and 19 tons of the corium of the melted core material was relocated to the lower head in the reactor vessel during the TMI-2 severe accident. However, the reactor vessel failure did not occur due to the operation of the HPI.

3. CINEMA Input Model and Steady State Results

The thermal power of the TMI-2 PWR was 2,772 MW_t. The TMI-2 core had 177 fuel assemblies, which had approximately 93 tons of fuel and 23 tons of the fuel cladding. The RCS of the TMI-2 included the reactor pressure vessel, two hot legs, the pressurizer including the surge line, two one-through steam generators, four RCPs, and four cold legs. The high pressure of the RCS in the TMI-2 was controlled by the pressurizer PORV. Figure 3 shows an input CSPACE model of the CINEMA computer code for the TMI-2. All RCS including the reactor vessel, two hot legs, the pressurizer, two steam generators, four RCPs and clod legs, pressurizer PORV, and HPI are modeled as shown in Figure 3. Three radial channels of central, middle, and outer for 177 fuel assemblies in the TMI-2, and 5 axial nodes of 1 to 5 are used in CSPACE core input model. Fuel and control rods for

Table 1: Detailed main events in TMI-2 severe accident.

Time (s)	Main events
0	Turbine and main feedwater pump trip
3	Pressurizer PORV valve opening
8	Reactor scram on high pressure signal
13	No pressurizer PORV valve closing
41	Operation of 1 (of 3) makeup pump 1B
122	HPI operation
278	Stop of HPI
480	Auxiliary feedwater startup
552	Core boiling begins
4,440	Shutdown B-loop RCP (end of phase 1)
6,000	Shutdown A-loop RCP
6,184	Core uncover
7,442	Cladding oxidation begins
7,719	Cladding failure
8,340	Close of the PORV line block valve
9,014	Fuel melting
10,440	Restart one B-loop RCP (end of phase 2)
11,580	Shutdown of the B-loop RCP
12,000	Start of primary system feed and bleed
13,440	Core material slumping (end of phase 3)
18,000	General emergency declared (end of phase 4)

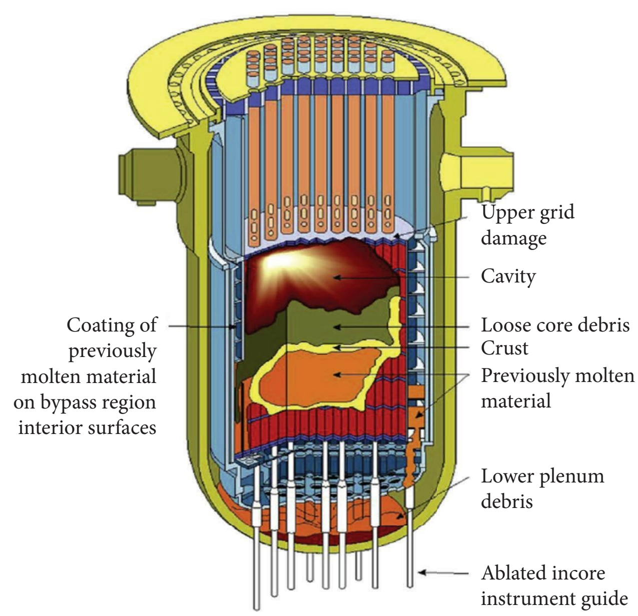

Figure 2: End state of TMI-2 severe accident.

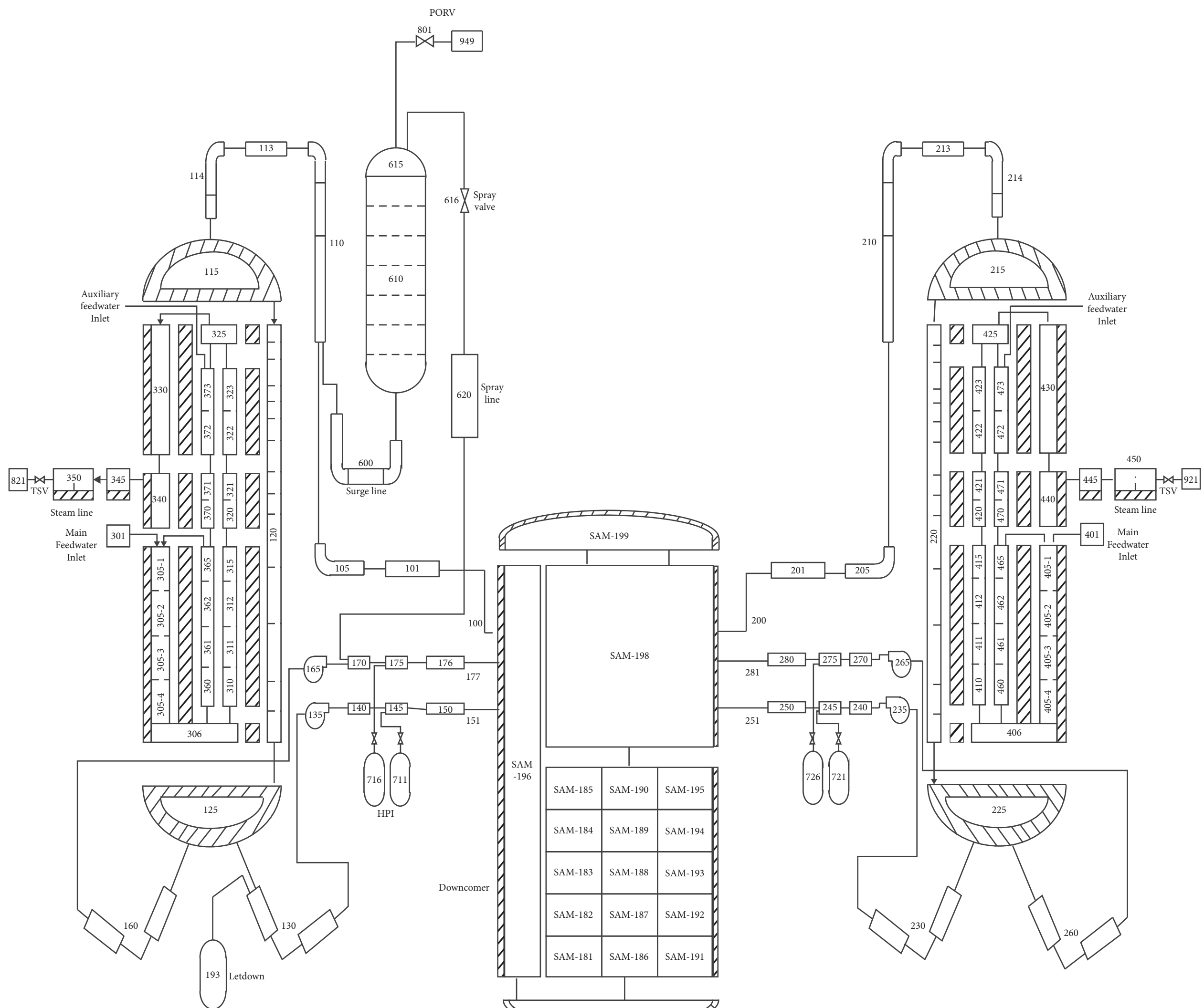

Figure 3: CINEMA modalization for TMI-2.

COMPASS model are connected to the SPACE fluid volumes in the core region.

A steady state simulation for approximately 2,000 s was performed to verify the input model of CINEMA computer code for TMI-2 severe accident. Table 2 shows a comparison of the CINEMA simulation results with the TMI-2 operating condition [13]. The steady state results of the CINEMA computer code for a selected set of parameters were in very good agreement with the TMI-2 operating conditions. The steady state results obtained from the CINEMA simulation were used as initial conditions for the TMI-2 transient calculation.

4. CINEMA Results and Discussion

Figure 4 shows the CINEMA results with the TMI-2 data on the pressurizer pressure. The total loss of feed water caused a dryout of the secondary side of the steam generators. This loss of heat sink capability of the RCS resulted in the coolant to expand and initially increased to/of the pressurizer pressure to opening setting point of the pressurizer PORV, which was 15.7 MPa. After the pressurizer PORV opened, the PORV failed to close as the pressurizer pressure decreased which resulted in RCS coolant loss through the PORV pipeline and initiated the SBLOCA. The HPI was operated by the SI (safety injection) signal. However, this actuation was stopped by operators who thought that the pressurizer water level indicated a nearly full of the RCS, while coolant continued to be lost through PORV pipeline. The pressurizer pressure remained at the saturation pressure of approximately 7 MPa for the primary system, after an initial decrease of the RCS pressure. After the fuel cladding temperature is higher than the saturation temperature, the pressurizer pressure increases by coolant boiling in the core. Increase of heat transfer from the fuel cladding to the coolant by decay and oxidation heats resulted in a coolant boiling and the pressurizer pressure to increase rapidly. The CINEMA results on the pressurizer pressure are very similar to the TMI-2 data in general. Moreover, the CINEMA results after molten pool formation and quenching at 10,440 s is not similar to the TMI-2 data

Table 2: Comparison of CINEMA results with the TMI-2 operating condition.

Parameters	Units	Design values	CINEMA results
Reactor power	MW	2700.0	2700.0
Coolant flow rate in core inlet	kg/s	16,804.8	16,404.6
Cold leg temperature	K	561.0	563.0
Hot leg temperature	K	592.0	595.0
Pressurizer pressure	MPa	15.2	15.2
Steam flow rate per SG (steam generator)	kg/s	718.0	717.0
Feed water flow rate per SG	kg/s	718.0	718.0
Feed water temperature at SG inlet	K	513.0	513.0
Steam pressure at SG outlet	MPa	7.2	7.1

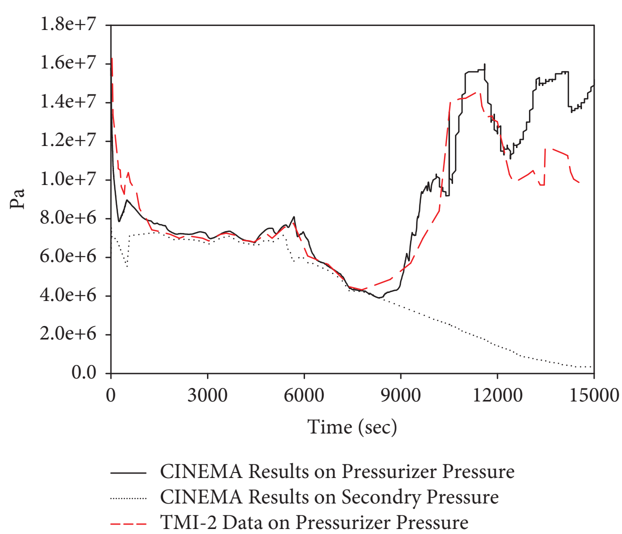

Figure 4: Comparison of CINEMA results with TMI-2 data on the pressurizer pressure.

because of complex quenching phenomena in the core by restart of the RCP and HPI operation.

Figure 5 shows the CINEMA results on mass flow rate through the pressurizer PORV in the TMI-2 severe accident. The opening of the pressurizer PORV at 3 s resulted in the mass flow rate through the PORV pipe line. In addition, the PORV failed to close led to loss of coolant through the PORV at approximately 10–30 kg/s of the coolant mass flow rate. After operator acted the close of the PORV line block valve at 8,340 s, the coolant mass flow rate reached to 0 kg/s. After the start of a feed and bleed operation for the primary system at 12,000 s, the coolant mass flow rate showed periodically peaks by the opening and closing of the PORV pipeline.

Figure 6 shows the CSPACE results of the CINEMA computer code on the collapsed water level for the pressurizer in the TMI-2 severe accident. When the pressurizer PORV opened, the collapsed water level increased to the top of the pressurizer because the coolant in the RCS moved to the pressurizer through the surge line. The collapsed water level decreased because of coolant loss through the PORV pipeline until 8,340 s. The pressurizer water drained to the RCS after the PORV block valve was closed, which resulted in the rapid decrease of the water level. After the start of HPI actuation by the feed and bleed operation of the primary system at 12,000 s, the water level increased. Figure 7 shows the CSPACE results of the CINEMA computer code on the collapsed water level for the core in the TMI-2 severe accident. After no PORV valve closing at 13 s, the water level decreased. The water level increased for short time after shutdown of A-loop RCP at 6,000 s. After restart, one B-loop RCP at 10,440 s and HPI operation at 12,000 s, the water level increased.

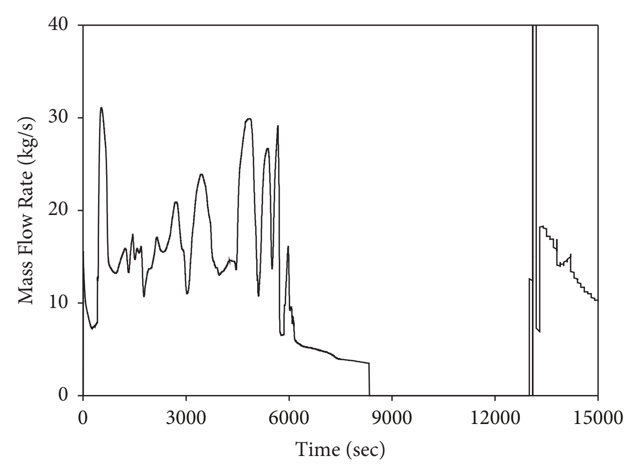

Figure 5: CINEMA results on mass flow rate through pressurizer PORV of the TMI-2 severe accident.

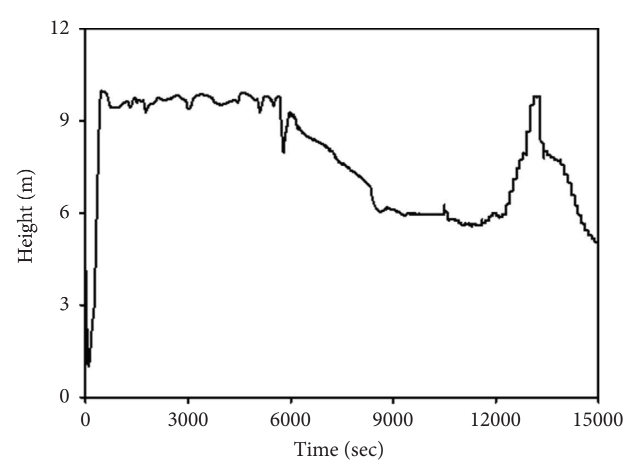

Figure 6: CINEMA results on collapsed water level in pressurizer of the TMI-2 severe accident.

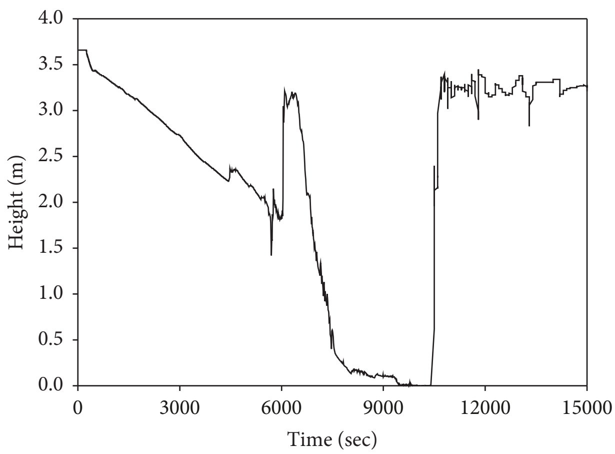

Figure 7: CINEMA results on collapsed water level in core of the TMI-2 severe accident.

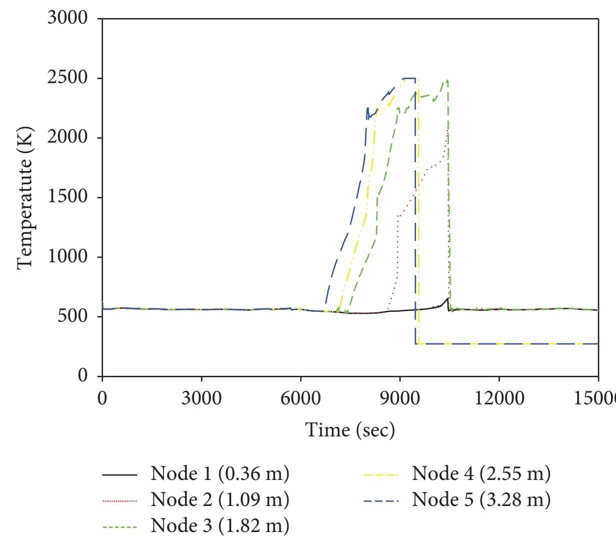

Figure 8: CINEMA results on fuel cladding surface temperature in TMI-2 severe accident.

Figure 8 shows the CINEMA results on fuel cladding surface temperature for the central channel. Position of nodes 1, 2, 3, 4, and 5 are 0.36 m, 1.09 m, 1.82 m, 2.55 m, and 3.28 m from the bottom of the fuel rod, respectively. The fuel cladding surface temperature is a little higher than the coolant temperature. Fuel cladding surface temperature at Node 5 rises when a core uncover occurs at the top of the core. The fuel cladding surface temperature rapidly increases by no quench of the core, which results in the damage of the fuel cladding and hydrogen production by the fuel cladding oxidation. When the fuel cladding temperature reaches approximately 1,000 K, fuel cladding oxidation begins. Following this time, the fuel cladding temperature rises abruptly due to the heat generation from oxidation. The fuel cladding surface temperature rapidly increases by no quench of the core, which results in the damage of the fuel cladding. The fuel cladding is quenched rapidly by water injection into the core at 10,440 s, which was occurred by RCP operation. Because of water in the bottom of the core as shown in Figure 7, the fuel cladding surface temperature at Node 1 did not increase. Figure 9 shows CINEMA results on the fuel cladding mass for the central channel in the core. Fuel cladding mass of only one fuel rod is in this Figure. The fuel cladding surface temperature rapidly increases by oxidation heat when the temperature reaches at approximately 1,500 K. Top of the fuel cladding (Node 4, 5) is melted and relocated to the middle part of the core (Node 2, 3). Fuel cladding surface temperature and relocation affect the hydrogen generation from the oxidation. The lowest value of the fuel cladding temperature after approximately 9,000 s means that all cladding is melted and relocated to the lower part.

Figures 10 and 11 show the CINEMA results on fuel of UO_2 temperature and mass for the central channel, respectively. Positions of nodes 1, 2, 3, 4, and 5 are same for fuel cladding cases. The fuel temperature rapidly increases by no quench of the core, which results in the damage of the fuel. The fuel is quenched rapidly by water injection into the core at 10,440 s, which was occurred by RCP operation. Fuel mass of only one fuel rod is in this figure. The fuel surface

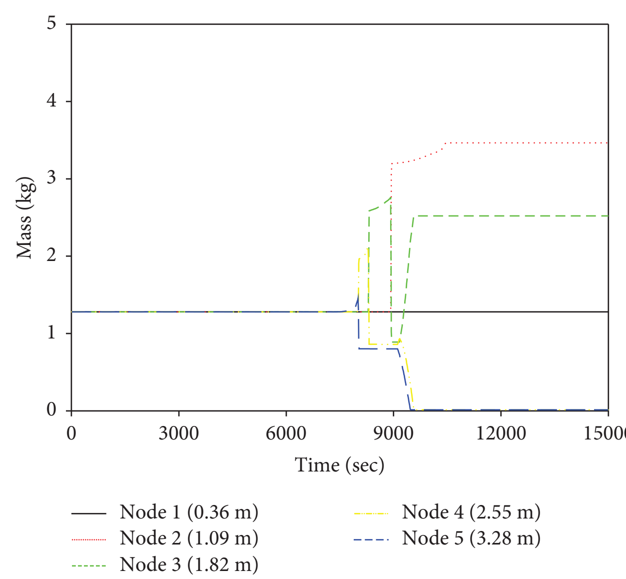

Figure 9: CINEMA results on fuel cladding mass in TMI-2 severe accident.

temperature rapidly increases by cladding oxidation heat. Top of the fuel (Nodes 4 and 5) is melted and relocated to the middle part of the core (Nodes 2 and 3). Zero value of the fuel mass after approximately 9,500 s means that in Node 5 all fuel is melted and relocated to the middle part. The upper part fuel rod of nodes 4 and 5 melts and relocates to the core middle part of the nodes 2 and 3, which is very similar to the melt pool formation in the real TMI-2 data, as shown in Figure 2.

Figure 12 shows a comparison of CINEMA results with TMI-2 data on the generated hydrogen mass. The calculated hydrogen generation mass is in general agreement with the hydrogen production estimated from the date base of the TMI-2 severe accident. The estimated hydrogen generation mass at the startup of the RCP was approximately 300 kg

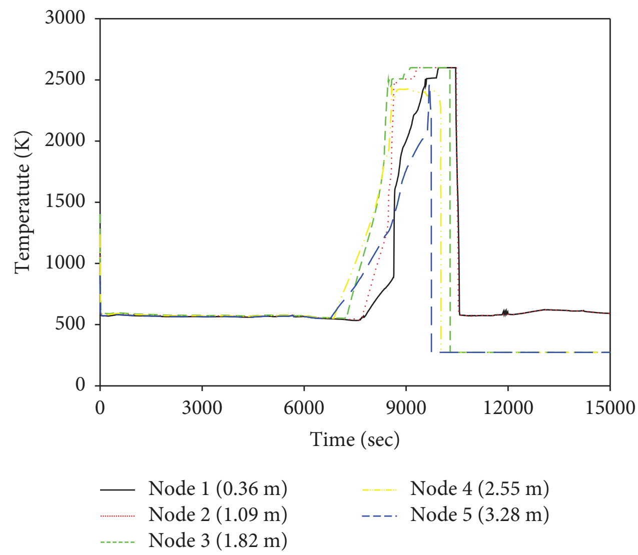

Figure 10: CINEMA results on fuel temperature in TMI-2 severe accident.

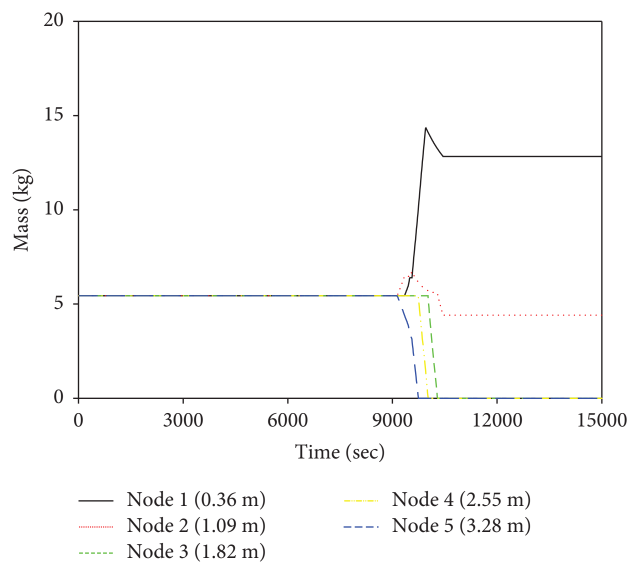

Figure 11: CINEMA results on fuel mass in TMI-2 severe accident.

[13]. At the startup of the RCP, the CINEMA calculations of cumulative hydrogen production are higher than 300 kg. However, the CINEMA results and measured total hydrogen generation mass are very similar, which were approximately 465 kg and 460 kg [13], respectively. Hydrogen production did not occur after 10,500 s because the intact fuel rods and some metallic cladding were quenched by the HPI water.

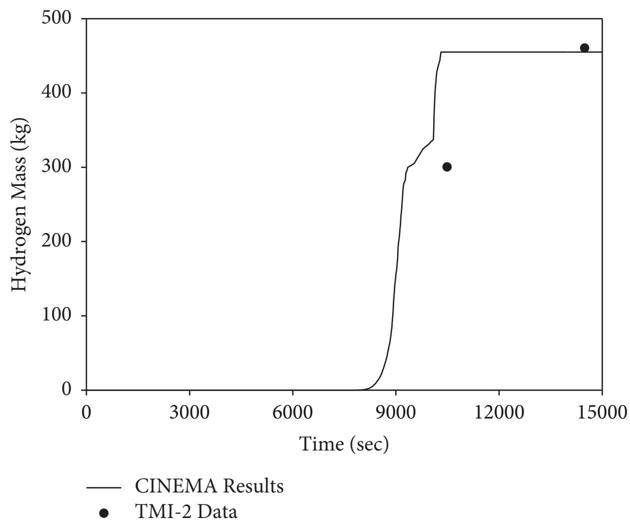

FIGURE 12: Comparison of CINEMA results with TMI-2 data on the generated hydrogen mass.

5. Conclusions

The severe accident progression in TMI-2 has been analyzed as a part of a validation of the CINEMA computer code, which is capable of simulating core melt progression with thermal hydraulic analysis of the RCS and severe accident analysis of the containment. The CINEMA results on main parameters, such as RCS pressure and an integrated hydrogen generation mass are compared with the TMI-2 data. The CINEMA results have shown that the RCS pressure is very similar to the TMI-2 data in general. The upper part of the fuel rod melts and relocates to the middle part of the core, which is very similar to the melt pool formation in the real TMI-2 data. The CINEMA results and measured total hydrogen production are very similar, which were approximately 465 kg and 460 kg, respectively. The CINEMA results after molten pool formation and quenching at 10,440 s is not similar to the TMI-2 data because of complex quenching phenomena in the core. For this reason, further CINEMA model development and analysis for a molten pool formation with crust formation and quenching process in the core and lower plenum of the reactor vessel are necessary to simulate all TMI-2 severe accident progression.

Data Availability

The published data used to support the findings of this study are included within the article.

Conflicts of Interest

The authors declare that they have no conflicts of interest.

Acknowledgments

This work was supported by the Korea Institute of Energy Technology Evaluation and Planning (KETEP) grant funded by the Korean government (Ministry of Trade, Industry, and Energy, Republic of Korea) (No. KETEP-20193110100050). This work was supported by the KETEP.

References

[1] Khnp, Kaeri, Fnc, and E. Kepco, "CINEMA user manual," 2018, https://assets.hisense-canada.com/assets/ProductDownloads/156/aaa06d21c2/AES-UMHS5660_Android_PHU100L5eng2020-v2.2.20MX.pdf.

[2] J. H. Song, D. G. Son, J. H. Bae et al., "CSPACE for a simulation of core damage progression during severe accidents," *Nuclear Engineering and Technology*, vol. 53, no. 12, pp. 3990–4002, 2021.

[3] Fnc, "SACAP user manual," 2017, https://www.sacap.edu.za/wp-content/uploads/2020/01/SACAP-Student-Handbook-2020-1.pdf.

[4] K. S. Ha, S. I. Kim, H. S. Kang, and D. H. Kim, *SIRIUS: A Code on Fission Product Behavior under Severe Accident*, Transactions of the Korean Nuclear Society Spring Meeting, Jeju, Korea, 2017.

[5] S. J. Ha, C. E. Park, K. D. Kim, and C. H. Ban, "Development of the SPACE code for nuclear power plants," *Nuclear Engineering and Technology*, vol. 43, no. 1, pp. 45–62, 2011.

[6] Khnp, E. Kepco, and C. Kaeri, "SPACE user manual," 2017, https://hypershop.zendesk.com/hc/en-us/articles/215810243-Space-user-manual.

[7] Khnp, E. Kepco, and C. Kaeri, "SPACE theoretical manual," 2017.

[8] J. H. Bae, D. G. Son, D. H. Kim et al., "Core degradation simulation of the PHEBUS FPT3 experiment using COMPASS code," *Nuclear Engineering and Design*, vol. 320, pp. 258–268, 2017.

[9] M. Z. Podowski, R. M. Podowski, D. H. Kim, J. H. Bae, and D. G. Son, "Compass - new modeling and simulation approach to PWR in vessel accident progression," *Nuclear Engineering and Technology*, vol. 51, no. 8, pp. 1916–1938, 2019.

[10] Sand2017-0445O, *MELCOR Computer Code Manuals, Vol. 1: Primer and Users' Guide*, US Nuclear Regulatory Commission, Rockville, MD, USA, 2018.

[11] Sand2017-0445O, *MELCOR Computer Code Manuals, Vol. 2: Reference Manual*, US Nuclear Regulatory Commission, Rockville, MD, USA, 2018.

[12] Fauske Associates, *MAAP5: Modular Accident Analysis Program for LWR Power Plants, Transmittal Document for MAAP5 Code Revision MAAP5.0.1*, Fauske Associates, Burr Ridge, IL, USA, 2011.

[13] J. P. Van Dorsselaere, C. Seropian, P. Chatelard et al., "The ASTEC integral code for severe accident simulation," *Nuclear Technology*, vol. 165, no. 3, pp. 293–307, 2009.

[14] B. J. Kim and S. W. Lee, "Development of dynamic motion models of SPACE code for ocean nuclear reactor analysis," *Nuclear Engineering and Technology*, vol. 54, no. 3, pp. 888–895, 2022.

[15] J. Ham, S. H. Kim, S. I. Kim et al., "Source term estimation under the SBLOCA-induced severe accident condition in the SMART," *Science and Technology of Nuclear Installations*, vol. 2021, Article ID 6686615, 14 pages, 2021.

[16] R. J. Park, J. Ham, S. H. Kim, S. I. Kim, B. Lee, and J. Kim, "Development of severe accident mitigation Technology and analysis for SMART," *Nuclear Engineering and Design*, vol. 374, Article ID 111061, 2021.

[17] S. Wu, Y. Zhang, D. Wang, W. Tian, S. Qiu, and G. Su, "Assessment of the severe accident code MIDAC based on

FROMA, QUENCH-06and16 experiments," *Nuclear Engineering and Technology*, vol. 54, no. 2, pp. 579–588, 2022.

[18] J. Bang, G. H. Choi, D. W. Jerng, S. W. Bae, S. Jang, and S. J. Ha, "Analysis of steam generator tube rupture accidents for the development of mitigation strategies," *Nuclear Engineering and Technology*, vol. 54, no. 1, pp. 152–161, 2022.

[19] R. J. Park, D. Son, H. S. Kang, S. M. An, and K. S. Ha, "Development of IVR-ERVC evaluation method and its application to the SMART," *Annals of Nuclear Energy*, vol. 161, Article ID 108463, 2021.

[20] M. S. Song, I. W. Park, E. S. Kim, and Y. G. Lee, "Numerical study on thermal-hydraulics of external reactor vessel cooling in high-power reactor using MARS-ks1.5 code: CFD-aided estimation of natural circulation flow rate," *Nuclear Engineering and Technology*, vol. 54, no. 1, pp. 72–83, 2022.

[21] D. K. Choi, W. M. Park, S. M. Son, K. Lim, Y. J. Cho, and C. Choi, "Numerical study of natural circulation flow in reactor coolant system during a severe accident," *Science and Technology of Nuclear Installations*, vol. 2022, Article ID 4531040, 17 pages, 2022.

[22] M. Annor-Nyarko, H. Xia, and A. Ayodeji, "Thermo-mechanical analysis of a reactor pressure vessel under pressurized thermal shock caused by inadvertent actuation of the safety injection system," *Science and Technology of Nuclear Installations*, vol. 2022, Article ID 886583, 14 pages, 2022.

[23] J. M. Broughton, P. Kuan, D. A. Petti, and E. L. Tolman, "A scenario of the three mile Island unit 2 accident," *Nuclear Technology*, vol. 87, no. 1, pp. 34–53, 1989.

[24] D. W. Akers, R. K. Mccardell, M. L. Russell, and G. Worku, "TMI-2 core materials and fission product inventory," *Nuclear Engineering and Design*, vol. 118, no. 3, pp. 451–461, 1990.

[25] T. Haste, J. Birchley, E. Cazzoli, and J. Vitazkova, "MELCOR/MACCS simulation of the TMI-2 severe accident and initial recovery phases, off-site fission product release and consequences," *Nuclear Engineering and Design*, vol. 236, no. 10, pp. 1099–1112, 2006.

[26] L. J. Siefken, D. T. Hagrman, and J. K. Hohorst, *SCDAP/RELAP5/MOD3.3 Code Manual, Appendix A*, US Nuclear Regulatory Commission, Rockville, MD, USA, 2001.